

# Jet: Multilevel Graph Partitioning on GPUs

Michael S. Gilbert\*

Kamesh Madduri<sup>†</sup>

Erik G. Boman<sup>‡</sup>

Sivasankaran Rajamanickam<sup>§</sup>

## Abstract

The multilevel heuristic is the dominant strategy for high-quality sequential and parallel graph partitioning. Partition refinement is a key step of multilevel graph partitioning. In this work, we present Jet, a new parallel algorithm for partition refinement specifically designed for Graphics Processing Units (GPUs). We combine Jet with GPU-aware coarsening to develop a  $k$ -way graph partitioner. The new partitioner achieves superior quality when compared to state-of-the-art shared memory graph partitioners on a large collection of test graphs.

## 1 Introduction

Parallel graph partitioning is a key enabler for both large-scale graph analytics [33, 37] and high-performance scientific computing [7, 34]. Graph partitioning [11] is the task of creating approximately equally-sized disjoint sets of vertices in the graph, while simultaneously minimizing the *cutsizes*, the number of edges connecting vertices in different sets. Most graph partitioning software and algorithms use the *multilevel* heuristic. The multilevel heuristic constructs a sequence of progressively smaller graphs in a *coarsening* phase, finds a solution to the problem (partitioning in this case) on the smallest graph, and then *uncoarsens* the solution to find the solution for the original graph. The uncoarsening step also *improves* the solution using information from each graph in the sequence in a process called *refinement*. At a high-level, refinement algorithms for graph partitioning work by *moving vertices* to improve the solution quality. The graph partition refinement problem is well-studied in the context of shared-memory algorithms for multicore systems [31, 3, 23]. Our work considers the problem of partition refinement on graphics processing units (GPUs), with a focus on matching

or exceeding partition quality obtained with fast multicore partitioners.

Our refinement algorithm, named Jet, decouples the two primary tasks of refinement algorithms: improving the cutsizes and maintaining a balanced solution. This enables our algorithm to move larger sets of vertices without relying too much on fine-grained synchronization. This is critical to obtaining a high-degree of parallelism. Moreover, we implement a novel heuristic for resolving conflicts between simultaneous vertex moves. This heuristic also enables our refinement to escape local minima. At a high level, the heuristic uses information from the current partition state to assign a priority value to each vertex, and then approximates the expected value for the next partition state from these priorities. The expected value for the next partition state in the neighborhood of each vertex determines whether the vertex should move. In addition to enabling larger sets of vertex moves, this results in higher quality than is possible with similar parallel refinement schemes on a majority of the test graphs we experimented with.

We develop a partitioner for GPUs utilizing a recent work in coarsening on the GPU [19] and the new Jet refinement algorithm. GPU acceleration enables our partitioner to achieve consistently faster partitioning times compared to other partitioners. Our partitioner also achieves consistently smaller cutsizes on graphs from varied domains such as finite element methods, social networks, and semiconductor simulations.

The following are the key algorithmic contributions and performance highlights:

- We present Jet, a novel high-quality, GPU-parallel,  $k$ -way refinement algorithm. Our experiments indicate that Jet outperforms the Multitry Local Search algorithm in terms of graph partition quality.
- We present a  $k$ -way graph partitioner that leverages GPU acceleration to attain  $2\times$  faster partitioning times than competing methods in a majority of test cases. We also modify the GPU implementation to adapt it for multicore execution.
- We demonstrate superior quality when compared

\*Pennsylvania State University, University Park, USA (msg5334@psu.edu).

<sup>†</sup>Pennsylvania State University, University Park, USA (madduri@psu.edu).

<sup>‡</sup>Sandia National Laboratories, Albuquerque, USA (egboman@sandia.gov).

<sup>§</sup>Sandia National Laboratories, Albuquerque, USA (srajama@sandia.gov).

to state-of-the-art shared memory partitioners on a diverse test set of 61 graphs.

## 2 Background and Prior Work

**2.1 Problem Definition** Consider a graph  $G$  with  $n$  vertices (or nodes) and  $m$  edges. We assume the graph is undirected and has no self-loops or parallel edges. Vertices can have associated positive integral weights. Edges weights are positive integers representing the strength of the connection of two vertices. The set of vertex-weight pairs are denoted by  $V$ , and the set of weighted edge triples by  $E$ . For a positive integer  $k$ , a  $k$ -way partition of  $G$  is a set of pairwise disjoint subsets of  $V$  (or *parts*  $\{p_1, p_2, \dots, p_k\} = P$ ) such that  $\cup_{i=1}^k p_i = V$ . The weight/size of a part  $p_i$  is the sum of the weights of its constituent vertices. Given a partition, the *cut set* is the set of edges  $\langle u, v, w_{uv} \rangle \in E$  with  $u$  and  $v$  in different parts. The sum of the weights of edges in the cut set is called the *cost* (or *cutsizes*, or *edge cut* in case of unweighted graphs) of the partition. A *balance constraint* in the form of a non-negative real constant  $\lambda$  places a limit on the part weights:  $\text{weight}(p_i) \leq (1 + \lambda) \frac{n}{k}$ ,  $\forall 1 \leq i \leq k$ ; there is no lower bound on the size of a part. The value of  $\lambda$  is typically 0.01–0.1 (or a 1–10% allowed imbalance). The objective of the  $k$ -way graph partitioning problem is to minimize the *cost* of the partition of  $G$  while satisfying the balance constraint. The output of the partitioning problem is typically an array of size  $n = |V|$  mapping vertices to the parts.

**2.2 Multilevel partitioning** The multilevel heuristic [41] is extensively used in large-scale graph analysis. Its applications include graph partitioning [25, 6, 28], clustering [15, 20, 18], drawing [29, 27], and representation learning [12, 4]. The family of algebraic multigrid methods [10, 42] and multilevel domain decomposition methods [40, 24] in linear algebra are closely related to multilevel methods for graph analysis. In a multilevel method, instead of solving a problem on a large graph, we build a hierarchy of graphs that are progressively smaller than the original graph and yet preserve the structure of the original graph. We then solve the problem on the smallest graph and *project* or *interpolate* the solution to the original graph using the hierarchy. Algorithm 1 gives the high-level template for multilevel graph partitioning. Refinement is applied after projection on each level during uncoarsening to reduce the *cutsizes*, and to satisfy the balance constraint if the coarser partition could not satisfy it.

Since there is a clear separation of multilevel coarsening, initial partitioning, and refinement in multilevel level partitioning, we focus on multilevel refine-

---

**Algorithm 1** A template for multilevel graph partitioning.

---

**Input:** graph  $G$  as defined in Section 2.1, number of parts  $k$ , balance  $\lambda$ .

**Output:** A partition array  $P_0[0..n - 1]$ , where  $P_0[v]$  indicates the partition that vertex  $v \in V$  belongs to.

```

1:  $\{G_0, \dots, G_l\}, \{M_0, \dots, M_l\} \leftarrow \text{MLCOARSE}(G)$ 
2:  $P_l \leftarrow \text{INITIALPARTITION}(G_l, k, \lambda)$ 
3:  $P_l \leftarrow \text{REFINEPARTITION}(G_l, P_l, k, \lambda)$ 
4:  $i \leftarrow l - 1$ 
5: while  $i \geq 0$  do  $\triangleright l$  Uncoarsening steps
6:    $P_i \leftarrow \text{PROJECTPARTITION}(P_{i+1}, M_{i+1})$ 
7:    $P_i \leftarrow \text{REFINEPARTITION}(G_i, P_i, k, \lambda)$ 
8:    $i \leftarrow i - 1$ 

```

---

ment in this work. Sequential and parallel algorithms for multilevel coarsening have been extensively studied [28, 36, 13, 19].

**2.2.1 GPU: Related Work** Most graph partitioners are designed for CPUs and do not run on GPUs. In particular, the refinement in the multilevel algorithm is difficult to parallelize on GPUs. The first GPU partitioner we are aware of was developed by Fagginger Auer and Bisseling [17]. They developed two algorithms for GPU: one multilevel spectral, and the other was multilevel with greedy refinement. Their code was never released. A later GPU partitioner [21] implemented a multilevel algorithm with a label-propagation based refinement algorithm.

Sphynx [2, 1] is a spectral partitioner that runs on multiple GPUs. It is not multilevel. Although it runs quite fast on GPUs, the cut quality is significantly worse (up to 50 $\times$ ) than Metis/ParMetis on irregular graphs. Therefore, we do not consider Sphynx any further in this paper.

**2.3 Refinement** The objective of the partition refinement problem is identical to graph partitioning. Refinement algorithms improve an input partition; in the multilevel method, this partition is an output from coarser levels in the multilevel hierarchy. It can also be used outside the context of multilevel partitioning, regardless of the method used to produce the given partition. Refinement is *local* in nature; information about the current partition state is used to generate the next state. Refinement methods frequently use a vertex attribute called the *gain*, which is defined according to the current partition state. For bipartitioning, the gain describes the decrease in *cutsizes* for moving a vertex from its current partition to the other partition. This

quantity is negative if the cutsize would increase. When  $k > 2$ , we use *gain* to indicate the expected decrease in cutsize for a *vertex move* (moving a single vertex from its current part to a specific destination part).

Refinement algorithms typically operate in *passes* over a set of vertices. The set can either be all vertices, or a subset of vertices such as the *boundary* set, or some other subset of interest. The number of passes is typically a small constant, and it is desirable that the running time of one refinement pass be linear in  $m = |E|$ . A vertex  $v$  is in the boundary set if there exists a vertex  $u$  in the neighborhood of  $v$  such that  $\text{part}(v) \neq \text{part}(u)$ . As no vertex outside the boundary set can have a positive gain vertex move, it is common for refinement passes to exclusively consider this set.

**2.4 Refinement: Related Work** In this work, we are interested in parallel partition refinement schemes. Several recent papers [30, 32, 31, 3] have demonstrated that parallel refinement techniques can obtain similar or better quality than sequential refinement algorithms. We group algorithms into four broad categories and describe them below.

**2.4.1 Label Propagation** Several refinement algorithms share similarities to an iteration of Label propagation (LP) community detection algorithm [35]. We thus group them into a common category. In these algorithms, the neighborhood of each vertex is examined to determine the part which the vertex is most connected to. The vertex is then moved into this part if doing so will not violate the balance constraint. A typical serial implementation visits each vertex of a graph at most once per iteration, in an arbitrary order. This technique is unable to escape local minima, which occur when no single vertex can be moved for a decrease in cutsize without violating the balance constraint. In parallel implementations, each processor owns a subset of the vertices, and each processor visits the vertices it owns in some order. A parallel implementation is synchronous if there is a barrier synchronization after all vertices are inspected in an iteration, or termed asynchronous if part changes are immediately applied. The balance constraint can be maintained in a parallel setting by atomically updating the part sizes. Mt-Metis [30], Mt-Kahip [3], and KaMinPar [23] all implement variations in a multilevel setting as a refinement option or the primary refinement method. PuLP [39] implements this technique for direct partitioning outside of a multilevel framework, using random initial partitions. The most recent GPU partition refinement algorithm [21] uses a synchronous scheme to construct a move buffer, which it subsequently consumes in small chunks.

**2.4.2 Hill-Scanning** Hill-scanning refinement [31] operates similar to greedy refinement [30], until it encounters a vertex with negative gain. It uses a priority queue (keyed on an approximation of the gain) to build a *hill* from the neighborhood of a seed vertex with negative gain, and terminates when the hill attains a positive gain value or becomes too large. Hills that don't attain positive total gain are discarded. Hill-scanning exploits parallelism by dividing the vertices among the processors, but a processor that is building a hill can use vertices owned by another processor.

**2.4.3 Multitry Local Search** The multitry local search (MLS) refinement algorithm attempts to find sequences of vertex moves that begin with a negative gain move, but produce a net improvement in the cutsize [3]. The algorithm consists of several global iterations, each consisting of several local iterations. Inside each local iteration, each processor consumes a thread-local priority queue seeded by some vertex and its neighborhood, and expands the priority queue to contain the neighborhood of all vertices it moves. Each processor begins with a new seed vertex when its queue is empty or it triggers a stopping rule. The seed vertices are consumed from a *todo list* initially containing all boundary vertices, but in successive local iterations the todo list contains only the vertices moved in the last local iteration.

**2.4.4 Network Flow Methods** Max-flow min-cut solvers have seen great success as partition refinement algorithms [38, 22]. Mt-KaHyPar creates a network flow problem by growing a region around the boundary between two parts. It uses a parallel implementation of the push-relabel algorithm to compute a minimum cut inside this region, and this new cut replaces the old cut if it satisfies the balance constraint. While flow-based methods outperform other refinement methods in terms of result quality, they are also considerably more expensive.

### 3 Our Partitioner

We now discuss our new multilevel GPU partitioner with an emphasis on the partition refinement algorithm. We perform coarsening until the coarsest graph obtained is extremely small, typically around 200 vertices. We use the  $k$ -way partitioning method in Metis [28] to perform the initial partitioning. Since the coarsest graph is very small, GPU parallelization of the initial partitioning is left for future work.

**3.1 Coarsening** Our coarsening approach is based on a GPU implementation discussed in [19], specifically

the *two-hop matching* approach originally developed for the Mt-Metis partitioner [32]. We modified the algorithm in [32] to further improve GPU execution efficiency.

**3.2 Kokkos** We use Kokkos [16] to implement the parallel kernels in our code. Kokkos facilitates performance portability, allowing the programmer to maintain a single-source program that can be compiled for different shared-memory architectures. We compile for three different targets: Nvidia GPUs using the CUDA toolkit, multicore CPUs using OpenMP, and single threads of the same CPUs using a serial backend. The Kokkos programming model involves expressing a task as a sequence of small kernels that fit one of three parallel primitives: parallel-for, reduction, and scan.

## 4 Jet Refinement Algorithm

We have two design goals for refinement on the GPU: matching or exceeding the quality of multicore refinement techniques, and running time that is comparable to fast multicore refinement. Prior shared-memory multicore-centric refinement algorithms such as hill-scanning and MLS rely on thread-local priority queues. Priority queues are necessary to find sequences of moves that improve the cutsizes where single moves cannot. However, these priority queue operations do not expose adequate concurrency for GPU-scale parallelism, and therefore such approaches are not viable on the GPU. Size-constrained LP-based refinement can visit the vertices in any order, and therefore lends itself naturally to both multicore and GPU parallelism. However, the size constraint limits the number of vertices that can be moved in each pass. This can be especially problematic if the distribution of beneficial moves is biased towards certain destination parts. To address this challenge, our method, Jet, splits a size-constrained LP iteration into two phases. The first phase is an unconstrained LP phase, Jetlp, that performs vertex moves while ignoring size constraints. The second phase is a rebalancing phase, Jetr, which has the task of moving vertices from oversized parts to non-oversized parts such that no oversized parts remain. It is paramount for the rebalancing phase to minimize any increase in cutsizes (or loss). LP-based algorithms generally produce lower-quality results than hill-scanning and MLS, and so we introduce novel augmentations to LP for improved quality. The overall structure of our refinement algorithm is to apply Jetlp until any part becomes oversized, then apply Jetr until balance is restored. We call each application of either Jetlp or Jetr as an “iteration”. We record the best balanced partition in terms of cutsizes, and terminate refinement when we exceed a

certain number of iterations (we use 12 for our results) without encountering a new best partition. We also use a tolerance factor  $\phi$  to terminate when the cutsizes are improving slowly.  $\phi$  is an important hyper-parameter to control the quality/runtime tradeoff, with  $\phi = 1$  prioritizing quality over runtime. We use  $\phi = 0.999$ , which appears to balance quality and runtime.

### 4.1 Unconstrained Label Propagation - Jetlp

Our unconstrained label propagation is synchronous, i.e., updates to the partition state are deferred to the end of each iteration. The steps in Algorithm 2 are as follows: first, a destination part  $P_d(v)$  is selected for each vertex  $v$ . Second, if  $P_d(v)$  is different from the current part  $P_s(v)$ , the vertex is pushed to an unordered list, and a priority is assigned. Finally, the algorithm filters this unordered list using an approximation of the expected value of the next partition state. It determines this approximation in the neighborhood of each vertex that passed the first filter, by merging  $P_s$  and  $P_d$  according to the priority values within each neighborhood. It performs all moves that pass the second filter, and then updates the data structures that track connectivity of each vertex and the sizes of each part. The name JET derives from a similarity in structure to a jet engine: the selection of destination parts is similar to the compressor, the first filter to the combustion chamber, and the second filter to the afterburner.

**4.1.1 Changes to address LP limitations** Most synchronous implementations of LP-based refinement have two limitations. First, it is not possible to improve cutsizes through negative gain vertex moves. Second, vertex moves in the same iteration can affect each other detrimentally. We introduce a method to address both of these problems: the *vertex afterburner*. The vertex afterburner is a heuristic-based conflict resolution scheme permitting negative-gain vertex moves. We use the term afterburner as it is applied to a list of vertex moves that may already be viable. Given a list of potential vertex moves  $X$ , we recompute the gain for each vertex in  $X$  according to an approximation of the next partition state in its neighborhood. This approximation is created by merging  $P_s$  with  $P_d$ , using an ordering *ord*. Due to the ordering *ord*, the approximations generated for overlapping neighborhoods are not consistent.  $P_d$  is fixed for all vertices in  $X$  prior to applying the afterburner, therefore recomputing the gain for each vertex  $v \in X$  only involves the parts  $P_d(v)$  and  $P_s(v)$  specific to the move. For each neighbor  $u$  of a vertex  $v \in X$ , if  $ord(u) < ord(v)$ , we calculate  $v$ 's gain assuming  $u$  will move to  $P_d(u)$ . Otherwise, we assume

---

**Algorithm 2** Jet - Label Propagation (Jetlp)

---

**Input:** The graph  $G = (V, E)$ . A partition array  $P_s$ . Data structures  $DS$  for querying vertex-part connection info and lock status

**Output:** A list of moves  $M$ , in the form of vertex-destination part pairs.

```
1:  $P_d \leftarrow P_s$ 
2:  $F \leftarrow \text{negativeInfinity}(|V|)$ 
3: for  $v \in V$  in parallel do
4:    $p_s \leftarrow P_s[v]$ 
5:    $A_v \leftarrow \text{adjacentParts}(v, DS) \setminus \{p_s\}$ 
6:   if  $A_v \neq \emptyset$  then
7:      $p_d \leftarrow \text{argmax}_{p \in A_v} \text{conn}(v, p)$ 
8:      $P_d[v] \leftarrow p_d$ 
9:      $F[v] \leftarrow \text{conn}(v, p_d) - \text{conn}(v, p_s)$ 
10:  $X, F \leftarrow \text{gainConnRatioFilter}(P_s, F, DS, c)$ 
11:  $X, F \leftarrow \text{removeLockedVertices}(X, F, DS)$ 
12:  $F_2 \leftarrow \text{zeros}(|X|)$ 
13: for  $v \in X$  in parallel do
14:    $p_s \leftarrow P_s[v]$ 
15:    $p_d \leftarrow P_d[v]$ 
16:    $f \leftarrow 0$ 
17:   for  $(u, w) \in E[v]$  in parallel do
18:      $p_u \leftarrow P_s[u]$ 
19:     if  $\text{ord}(u) < \text{ord}(v)$  then
20:        $p_u \leftarrow P_d[u]$ 
21:     if  $p_u = p_d$  then
22:        $f \leftarrow f + w$ 
23:     else if  $p_u = p_s$  then
24:        $f \leftarrow f - w$ 
25:    $F_2[v] \leftarrow f$ 
26:  $M \leftarrow \text{removeNegatives}(X, P_d, F_2)$ 
27:  $DS \leftarrow \text{resetLocks}(DS)$ 
28:  $DS \leftarrow \text{setLocks}(DS, M)$ 
```

---

$u$  remains in  $P_s(u)$ . This allows for vertex moves which initially had negative gain to become positive gain, and vice versa, depending on the other moves in  $X$ . The final move list  $M$  is chosen as a subset of  $X$ , containing only the moves in  $X$  with non-negative gain after recalculation. Let  $F(x) = \text{conn}(x, P_d(x)) - \text{conn}(x, P_s(x))$  be the priority values for each vertex move, given by the gain values of each vertex move in a vacuum.  $\text{ord}$  is defined as follows:

$$(4.1) \quad \begin{cases} \text{ord}(u) < \text{ord}(v) & u \in X \wedge F(u) > F(v) \\ \text{ord}(u) < \text{ord}(v) & u \in X \wedge F(u) = F(v) \wedge u < v \\ \text{ord}(u) > \text{ord}(v) & \text{otherwise} \end{cases}$$

**4.1.2 Negative Gain Moves** The efficacy of this filter heuristic is sensitive to the composition of  $X$ . If  $X$  is selected too conservatively (i.e., only positive gain vertex moves), then afterburning produces no additional benefit over standard LP. If  $X$  is unconstrained (i.e., the entire boundary vertex set), then afterburning will produce worse results than standard LP. To determine the composition of  $X$ , we must first determine a value  $P_d(v)$  for each vertex  $v$ :

$$(4.2) \quad P_d(v) = \text{argmax}_{p \in P \setminus \{P_s(v)\}} \text{conn}(v, p)$$

If a vertex is only connected to  $P_s(v)$ , it is not a boundary vertex and therefore is always excluded from  $X$ . The criterion for a vertex to be selected into  $X$  is as follows:

$$(4.3) \quad -F(v) < \lfloor c \cdot \text{conn}(v, p_s) \rfloor$$

$c$  is a constant that can be adjusted for different levels of the multilevel hierarchy. We find experimentally that 0.25 is most effective for the finest level of the hierarchy, whereas  $c = 0.75$  is best for all other levels (for our partitioner). It is important to note the floor rounding, as our results on certain graphs are sensitive to the rounding direction. We find that the coarsening and initial partitioning algorithms affect the optimal choice for  $c$ .

**4.1.3 Vertex Locking** We employ an additional technique that is intended to help migrate the boundary in a coordinated fashion across successive iterations. This technique employs a lock bit, which excludes all vertices selected into  $M$  by an iteration of our LP from being chosen into  $X$  in the next iteration of our LP. Locking helps to prevent oscillations, which occur when a vertex moves back and forth between two parts in successive iterations. These oscillations may decrease solution quality by increasing the difficulty in changing the boundary's shape and location.

## 4.2 Rebalancing - Jetr

**4.2.1 Two parts** We introduce rebalancing with a simpler version applicable only when  $k = 2$ . Without loss of generality, let  $p_a$  be the overweight part, and let  $p_b$  be the other part. The goal of our rebalancing is to move vertices from  $p_a$  to  $p_b$  until  $p_a$  is no longer overweight, while minimizing the increase in the cutsizes. We assign a simple loss value to every vertex in  $p_a$ :  $\text{loss}(v) = \text{conn}(v, p_a) - \text{conn}(v, p_b)$ . We order the vertices of  $p_a$  in terms of increasing loss as a sequence  $L$ . We then select the prefix  $L_x$  of  $L$  that minimizes the following value:

$$(4.4) \quad ||L_x| - (|p_a| - |p_b|)|$$

It is expensive to use a sort to obtain  $L$ , so we approximate  $L$  with  $L'$ , where vertices are binned according to a loss value. The bins are derived from the following equation:

$$(4.5) \quad \text{slot}(v) = \begin{cases} 2 + \lfloor \log_2(\text{loss}(v)) \rfloor & \text{loss}(v) > 0 \\ 1 & \text{loss}(v) = 0 \\ 0 & \text{loss}(v) < 0 \end{cases}$$

We find experimentally that the frequency of loss values tends to decrease as the absolute value of the loss value increases. We use  $\log_2$  to assign slot values so that there are more slots closer to zero than far away from zero. This semi-ordering is similar to a bucketing approach used for computing the top  $k$  elements in a vector [5], but it only approximates the top  $k$  elements to save time. The insertion order within each bucket is subject to race conditions. To reduce the atomic contention on GPU for the size counters of each bucket, we create  $\rho$  sub-buckets within each bucket that are keyed by  $v \bmod \rho$ . This bucket-oriented approach also integrates well when computing lists for multiple overweight parts independently in our  $k > 2$  variations.

Let  $L'_x$  be the prefix of  $L'$  that minimizes equation 4.4. In a graph with uniform vertex weights, the following inequality applies if  $\exists v \in L_x(\text{loss}(v) \geq 0)$ :

$$(4.6) \quad \sum_{v \in L'_x \setminus L_x} \text{loss}(v) \leq 2 \sum_{v \in L_x \setminus L'_x} \text{loss}(v)$$

**4.2.2 More than two parts** Extending the rebalancing formulation for the general case is non-trivial. We propose two separate extensions for an arbitrary  $k$  that both reduce to the  $k = 2$  formulation. Similar to label propagation, the output consists of an unordered list of vertices to move and their chosen destinations. The first formulation uses the following definition of loss:

$$(4.7) \quad \text{loss}(v) = \max_{p_b \ni |p_b| < \sigma} \text{conn}(v, p_b) - \text{conn}(v, p_a)$$

$\sigma$  determines the maximum size for a part to be considered a valid destination, and is chosen such that there is a deadzone between the size of valid destination parts and the size of oversized parts. In this formulation, vertices are evicted from the oversized parts such that each oversized part is just smaller than the size limit (this should be within the deadzone). This process is similar to the  $k = 2$  formulation, except that there are multiple oversized parts. Evicted vertices are sent to their best connected part among the valid destination parts. It is possible that the vertex is not connected to any valid destination part, in which case a random valid destination is chosen. Destination parts may become oversized.

However, the deadzone prevents oversized parts from becoming valid destinations. This guarantees at most  $k$  iterations to achieve a balanced partition, as at least one part will move into the deadzone in each iteration if vertex weights are uniform. We observe that the typical number of iterations required is substantially less than  $k$ . We denote this extension as weak rebalancing (Jetrw) due to the potential need for many iterations.

Our second extension uses the following definition of loss:

$$(4.8) \quad \text{loss}(v) = \text{mean}_{p_b \ni |p_b| < \sigma} \text{conn}(v, p_b) - \text{conn}(v, p_a)$$

Vertices are evicted from oversized parts in the same manner as the prior formulation. The destination parts then try to acquire as close to  $\sigma - |B|$  vertices from the evicted set as possible. Given that the evicted vertices are arranged in an unordered list, each destination partition selects a contiguous group from this list. Destination partitions are overlaid onto the unordered list according to their capacity, forming a one-dimensional “cookie-cutter” pattern. This formulation guarantees that no oversized parts remain after a single iteration, if vertex weights are unit. We observe that vertex weights are often a significant fraction of the size constraint when more than one iteration is necessary. We denote this extension as strong rebalancing (Jetr) due to its ability to achieve balance in one iteration in most scenarios.

Jetrw is much more effective at minimizing loss than Jetr, even though it may require more iterations to converge upon a balanced partition. Our observations indicate that Jetr requires fewer iterations to converge in any of the following scenarios: regular graphs, small values of  $k$ , and large imbalance ratios. We propose a combination of the two formulations, wherein we apply Jetrw for a certain number of iterations, and then apply Jetr if the partition is still unbalanced. We find that even a single iteration of Jetrw followed by an iteration of Jetr can achieve much of the benefit of a large number of iterations of Jetrw. Our full rebalancing (Jetr) consists of two iterations of Jetrw followed by a single iteration of Jetr. If more iterations are necessary due to large vertex weights, these are performed with Jetr. For both rebalancing variants, we find it beneficial to restrict a vertex from leaving an oversized partition if its respective vertex weight is larger than  $1.5(|p_a| - \frac{|V|}{k})$ . This restriction is applied before we construct  $L'$ .

**4.3 Data Structures and Optimization** We represent our input graphs and coarse graphs in-memory using the compressed-sparse-row (abbreviated as CSR) format. We require a data structure to track connectiv-

ity of each vertex to each partition in order to facilitate Jet’s iterations. Our label propagation iterations must be able to quickly identify the first and second most connected parts for each vertex. Our weak rebalancing iteration must identify the most connected valid destination part for each vertex in an oversized part. Our strong rebalancing iteration must sum the connectivity among valid destination parts for each vertex in an oversized partition. Finally, it should be possible to modify this data structure given a list of vertices to move. A naive implementation might use  $O(k|V|)$  space to explicitly track this connectivity data for each possible pair of a vertex and part. Unfortunately, this uses far too much space with otherwise reasonable values for  $k$ , and is inefficient to traverse in all use cases. Our implementation builds on the observation that for any vertex  $v$ , the number of partitions to which it can have nonzero connectivity is at most  $\min(k, \text{degree}(v))$ . We utilize a formulation similar to the CSR graph format to represent the vertex-part connectivity matrix. Our data structure allocates space equal to the following equation:

$$(4.9) \quad |V| + 2 \sum_{v \in V} \min(k, \text{degree}(v))$$

Each row in this CSR representation is treated as a hash table (keyed on the partition id) for creation and updates. To determine the most connected parts that satisfy some filter criteria respective to each use case, we linearly search the hash tables. This linear search is substantially more efficient for smaller hash tables, so we limit the number of empty entries. Although  $\min(k, \text{degree}(v))$  is the maximum possible part connections for each vertex, we observe that many graphs (particularly regular graphs but even many irregular graphs) have a much smaller number of nonzero connections in practice. For instance, it is possible for a degree=100 vertex with  $k = 128$  to only have one or two nonzero part connections. We set the hash table size to be slightly larger than the initial connectivity upon construction. This may cause insertions into the hash table to fail once this limited capacity is reached. When this occurs, we expand the hash table capacity and recalculate its contents. We assign a small amount of extra space to each hash table to limit the frequency that this is necessary.

## 5 Experimental Setup

Our experiments evaluate the performance of our partitioner in terms of both cutsizes and overall runtime. We compare to other state-of-the-art parallel partitioners including Mt-Metis v0.7.2 with Hill-Scanning, Mt-KaHIP v1.00 with MLS, and KaMinPar v1.0, as well

as the serial partitioner Metis v5.1.0. We are unable to compare with either other GPU partitioner [17, 21], as their code is unavailable. In the later work [21], their cutsizes results were slightly worse than both Metis and Mt-Metis (without Hill-Scanning) on all graphs tested. We evaluate on  $k = 32$ ,  $k = 64$ ,  $k = 128$  and  $k = 256$  with imbalance set to 3%, as well as  $k = 128$  with imbalance set to 1% and 10%. This constitutes a total of six experiments per graph and partitioner. Although our partitioner can operate on arbitrary values of  $k$ , Mt-KaHIP cannot, therefore our experiments are on  $k$  values that are powers of 2. For each combination of graph, experiment, and partitioner, we collect the median cutsize and median runtime across a number of runs. The number of runs performed is dependent on the partitioner: we perform five runs for Mt-KaHIP MLS, 11 runs for KaMinPar and Mt-Metis HS, three runs for Metis, and 21 runs for our partitioner. We present breakdowns versus each opposing partitioner by experiment configuration, and in terms of graph classification. The full version of this paper contains results directly evaluating the Jet refinement algorithm versus the MLS refinement algorithm, as well as parallel scaling results.

**5.1 Test Graphs** Our test set contains all graphs with at least 50 million nonzeros but less than 750 million nonzeros from the Suitesparse graph repository [14] (excluding the mawi graphs). We additionally include a few miscellaneous graphs (ppa, citation, products) from Open Graph Benchmark [26] and some social networks (dblp10, amazon08, hollywood11, enwiki21) published by the Laboratory for Web Algorithms [9, 8]. We also add a 2000x4000 rectangular mesh (grid), and a 200x200x200 cubic mesh (cube). We preprocess all graphs by performing the following steps: we remove self-loops, convert all directed edges to undirected edges, remove duplicate edges, and extract the largest connected component. The graphs are further grouped into one of nine classes. Table 1 lists all the graphs. Within each class, the graphs are ordered in the increasing order of number of edges after preprocessing.

**5.2 Test Systems** We conduct our tests on two different systems. The first system features a 32-core AMD Ryzen 3970x “Threadripper” processor with 256 GB of RAM (quad-channel DDR4). We use this system for all of our multicore tests. We run our partitioner and competing partitioners using 64 software threads on this system. The second system is a virtual instance with 12 virtual cores of an Intel Xeon Gold 6342 CPU, 90 GB RAM, and an Nvidia A100 GPU with 80 GB

Table 1: The complete set of graphs used in performance evaluation.

Category	Count	Graphs
Web crawl	4	wbEdu, ic04, uk02, arabic05
Social network	12	dblp10, amazon08, socPocec, citation, comLiveJournal, socLiveJournal, ljournal08, hollywood09, products, hollywood11, orkut, enwiki21
Semiconductor	4	circuit5M, vasStokes2M, vasStokes4M, stokes
Road network	2	roadUSA, europeOSM
Optimization	3	nlpkkt120, nlpkkt160, nlpkkt200
Finite element	15	feRotor, afShell, Hook1498, Geo1438, Serena, audikw, channel050, Long-Coup, dielFilterV3, MLGeer, Flan1565, Bump2911, CubeCoup, HV15R, Queen4147
Biology	7	ppa, cage15, kmerV2a, kmerU1a, kmerP1a, kmerA2a, kmerV1r
Artificial mesh	10	grid, cube, delaunay23, bubbles00, bubbles10, rgg22, bubbles20, delaunay24, rgg23, rgg24
Artificial complex	4	kron20, mycielskian17, kron21, mycielskian18

of VRAM. Both systems run Ubuntu 20.04. We report results with the A100 GPU for our partitioner. Our code is compiled with NVCC using CUDA Toolkit version 11.6.2 for the A100 platform, and GNU g++ version 10.2.0 on the ThreadRipper 3970x platform. We use release versions 3.6.1 of both Kokkos and Kokkos-Kernels libraries.

## 6 Partitioner Performance Evaluation

**6.1 Partitioning Quality** We first provide a summary comparison of our partitioner to four methods – Mt-KAHIP MLS, KaMinPar, Mt-Metis HS, Metis – in Table 2 for the six partitioning configurations. For all configurations, the geometric means of edge cut ratios indicate that our method outperforms competitors. Overall, we find that our partitioner performs better on about 70% of instances when compared to Mt-KaHIP MLS, more than 80% of instances versus KaMinPar, and more than 90% of test instances than Mt-Metis HS and Metis. When keeping the imbalance at 3% and varying the number of parts, we find that the quality with respect to Mt-KaHIP MLS does not change much, but our partitioner appears to have an advantage for lower values of  $k$  versus the other three partitioners. When varying the imbalance while keeping the number of parts the same ( $k = 128$ ), our partitioner outperforms Metis and Mt-Metis HS by a larger margin for larger imbalance factors.

Next, we identify our partitioner’s strengths and weaknesses by breaking down the input instances by graph class in Figures 1a and 1b. Our partitioner is dominant on finite element problems, optimization problems, social networks, semiconductor problems, and artificial complex networks. Of the social networks,

our partitioner only failed to produce the best cut on amazon08 and dblp10, which are the two smallest social networks in our test set. We have a moderate strength on biology graphs, with Mt-KaHIP beating us on the two smallest kmer graphs, and Metis beating us on the largest kmer graph. Our weaknesses include the artificial meshes, web crawls, and road networks. Excluding the web crawls, most of the graphs in these classes have an underlying 2D structure.

**6.2 Jet evaluation** In Table 3, we evaluate the impact of the design choices in our JET LP phase in comparison to a baseline synchronous LP. Our baseline only moves vertices into their best connected partition, omits the afterburner kernel in its entirety, and ignores the lock bit. We compare four versions of the LP phase. The first alternate is the baseline plus vertex locking. The second alternate is the baseline plus a weaker version of the afterburner, that only considers vertex moves with positive or zero gain. The third alternate is the baseline plus the full afterburner, ie. it considers negative gain vertices as described in section 4.1.2. The fourth version is the full JETlp algorithm, ie. the baseline plus vertex locking plus the full afterburner. The results in Table 3 show that the afterburner performs substantially better if it can consider negative gain vertex moves than if it can’t. Interestingly, the vertex lock doesn’t provide any benefit by itself, but combined with the full afterburner it provides a benefit of 2.2% versus the full afterburner without the locks. We additionally investigate the impact of  $\phi$  on the runtime and cutsizes results of our final version. We found decreasing our refinement tolerance value  $\phi$  to 0.99 improves uncoarsening time by 56% and worsens the cutsizes by 1.1% over our default value of 0.999. Increasing  $\phi$  to 0.9999 worsens the uncoarsening

Table 2: We compare Jet to various partitioners, reporting the ratios of the geometric means of median cutsizes obtained with the partitioner to the median cutsize with Jet. A value greater than 1 indicates that Jet performs better. The number of parts and the balance constraint setting are varied.

<i>Partitioner</i>	<i>k</i> = 32	<i>k</i> = 64	<i>k</i> = 128	<i>k</i> = 256	<i>k</i> = 128	<i>k</i> = 128	<i>Overall</i>
	<i>i</i> =3%	<i>i</i> =3%	<i>i</i> =3%	<i>i</i> =3%	<i>i</i> =1%	<i>i</i> =10%	
Mt-KaHIP MLS	1.020	1.020	1.022	1.021	1.043	1.026	1.025
KaMinPar	1.084	1.074	1.063	1.049	1.067	1.073	1.068
Mt-Metis HS	1.111	1.094	1.084	1.073	1.075	1.100	1.089
Metis	1.099	1.085	1.072	1.063	1.069	1.088	1.079

time by 33% and improves the cutsizes by 0.5% over the default value.

Table 3: We compare a baseline version of Jet and progressively add optimizations, reporting the geometric means of the cutsizes ratios obtained in each case. A value greater than 1 indicates an improvement in cutsizes.

Variant	Ratio
Baseline + Locks	1.000
Baseline + Weak Afterburner	1.009
Baseline + Full Afterburner	1.030
Full JET	1.052

**6.3 Overall execution time** As we show in Figure 2a, our partitioner achieves strong runtime results on artificial complex, biology, road network, semiconductor, and social network graphs. Our partitioner achieves similar runtime performance to Mt-Metis HS on the finite element graphs, and it also achieves similar performance to KaMinPar on the web crawl graphs. The runtime performance of Mt-KaHIP is surprising; in Figure 2b, we see that it is faster than Metis (which is sequential) on only the  $k = 32$  and  $k = 64$  configurations. In the same figure, our partitioner shows similar performance trends across experiment configurations.

Overall, our GPU partitioner is consistently faster than CPU competitors, with shorter runtimes than any competitor in over 85% of test instances. We find that our partitioner was faster than Mt-KaHIP MLS on over 99% of test instances, and more than twenty times faster in over 40% of test instances. In comparison to KaMinPar, our partitioner is faster in over 90% of instances and at least twice as fast in over 65% of instances. Versus Mt-Metis HS, our runtime was better in over 90% of test instances, and at least twice as fast in over 60% of instances. Our partitioner is more than 20× faster than Metis in over 40% of test instances,

similar to Mt-KaHIP MLS.

In Table 4, we present the average time spent in each subtask of partitioning by our graph partitioner on the GPU. Across all classes, initial partitioning is responsible for at most 10.6% of the total runtime. Coarsening dominates on artificial complex, semiconductor, and web crawl graphs, whereas uncoarsening dominates on the other graphs. Coarsening tends to dominate on most graphs where the degree distributions are irregular, whereas uncoarsening dominates on the more regular graphs.

Table 4: Percentage partitioning time by subtask.

Graph class	Uncoarsen	Coarsen	InitPart
Web Crawl	30.3	64.6	5.1
Social Network	58.2	31.2	10.6
Semiconductor	38.9	56.2	4.9
Road Network	54.0	42.3	3.7
Optimization	50.4	45.3	4.3
Finite Element	55.4	34.9	9.7
Biology	63.9	28.3	7.9
Artificial Mesh	64.6	31.2	4.2
Artificial Complex	36.9	54.7	8.4

## 7 Conclusion

We develop a graph partitioning method that leverages GPU acceleration to decrease overall partitioning time, while delivering state-of-the-art partition quality. Our partitioner demonstrates superior quality on six of nine graph classes in our test set compared to four state-of-the-art partitioners, across six experiment configurations. Our runtimes are superior on all nine graph classes. We attribute these results primarily to our novel partition refinement algorithm, Jet. Jet builds on label propagation by addressing many common drawbacks, while optimizing for GPU scalability. Our partitioner is able to substantially reduce the time spent for initial partitioning by coarsening to extremely small graphs.

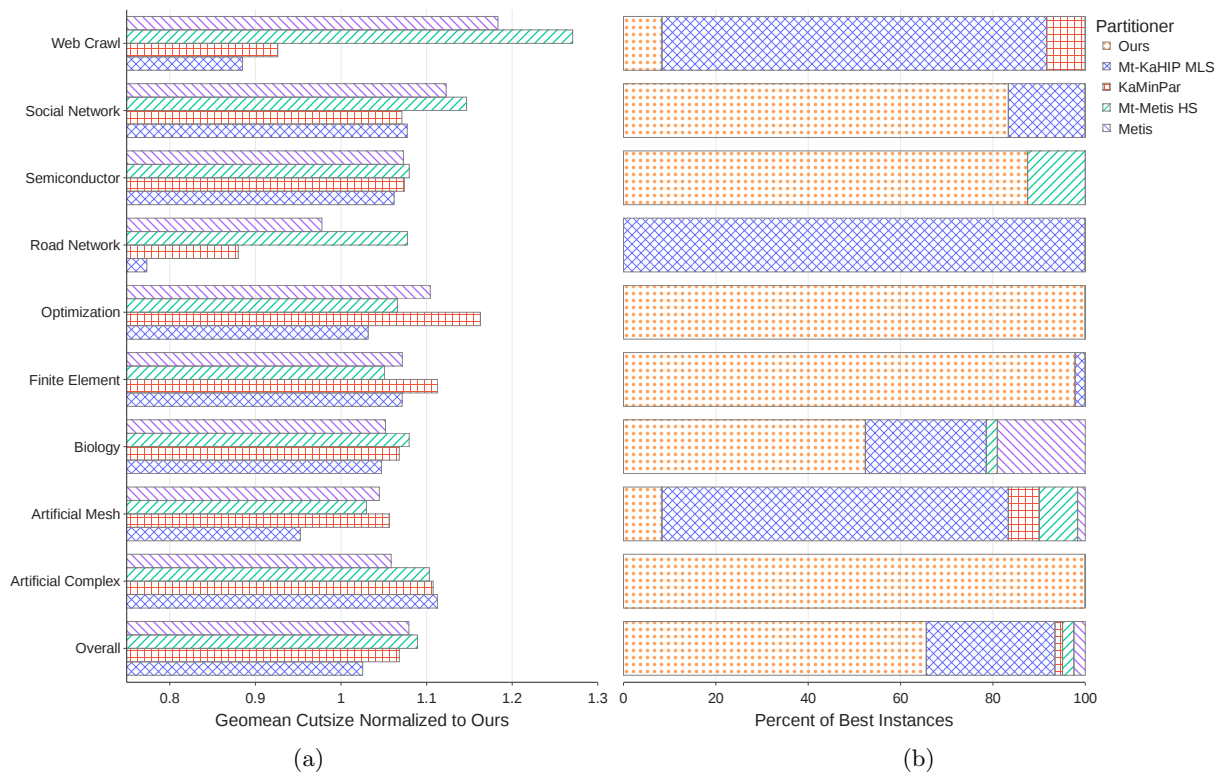


Figure 1: Cutsizes Results By Graph Class

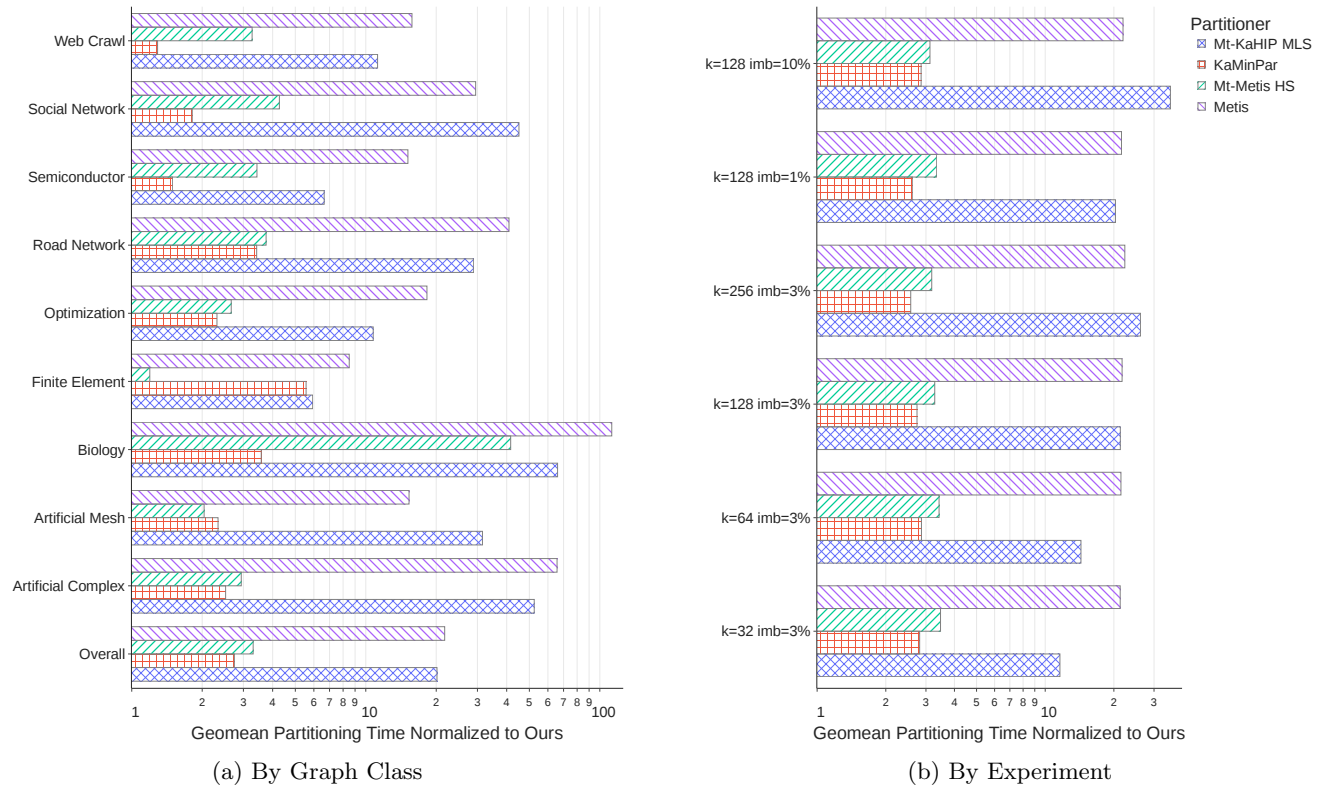


Figure 2: Partitioning Time Comparison

In future work, we plan to investigate graph learning to enhance the Jet afterburner heuristic. We also plan to adapt Jet and our partitioner for multilayer network partitioning, multi-constraint partitioning, and multi-GPU execution.

## Acknowledgments

Sandia National Laboratories is a multimission laboratory managed and operated by National Technology and Engineering Solutions of Sandia, LLC., a wholly owned subsidiary of Honeywell International, Inc., for the U.S. Department of Energy’s National Nuclear Security Administration under contract DE-NA-0003525. This research was supported by the Exascale Computing Project (17-SC-20-SC), a collaborative effort of the U.S. Department of Energy Office of Science and the National Nuclear Security Administration.

## References

- [1] S. Acer, E.G. Boman, C.A. Glusa, and S. Rajamanickam, *Sphinx: A parallel multi-GPU graph partitioner for distributed-memory systems*, *Parallel Computing*, 106 (2021), p. 102769, <https://doi.org/10.1016/j.parco.2021.102769>.
- [2] S. Acer, E.G. Boman, and S. Rajamanickam, *SPHYNX: Spectral Partitioning for HYbrid aNd aXelerator-enabled systems*, in *Proc. Int’l. Parallel and Distributed Proc. Symp. Workshops (IPDPSW)*, 2020.
- [3] Y. Akhremtsev, P. Sanders, and C. Schulz, *High-quality shared-memory graph partitioning*, *IEEE Transactions on Parallel and Distributed Systems*, 31 (2020), pp. 2710–2722.
- [4] T.A. Akyildiz, A.A. Aljundi, and K. Kaya, *GOSH: Embedding big graphs on small hardware*, in *Proc. Int’l. Conf. on Parallel Processing (ICPP)*, 2020.
- [5] T. Alabi, J.D. Blanchard, B. Gordon, and R. Steinbach, *Fast k-selection algorithms for graphics processing units*, *ACM J. Exp. Algorithmics*, 17 (2012), <https://doi.org/10.1145/2133803.2345676>.
- [6] S.T. Barnard and H.D. Simon, *Fast multilevel implementation of recursive spectral bisection for partitioning unstructured problems*, *Concurrency: Practice and Experience*, 6 (1994), pp. 101–117.
- [7] R.H. Bisseling, *Parallel Scientific Computation: A Structured Approach Using BSP*, Oxford University Press, USA, 2020.
- [8] P. Boldi, M. Rosa, M. Santini, and S. Vigna, *Layered label propagation: A multiresolution coordinate-free ordering for compressing social networks*, in *Proc. 20th Int’l. Conf. on the World Wide Web (WWW)*, 2011, pp. 587–596.
- [9] P. Boldi and S. Vigna, *The WebGraph framework I: Compression techniques*, in *Proc. 13th Int’l. World Wide Web Conf. (WWW)*, ACM Press, 2004, pp. 595–601.
- [10] A. Brandt, *Algebraic multigrid theory: The symmetric case*, *Applied mathematics and computation*, 19 (1986), pp. 23–56.
- [11] A. Buluç, H. Meyerhenke, I. Safro, P. Sanders, and C. Schulz, *Recent advances in graph partitioning*, *Algorithm engineering*, (2016), pp. 117–158.
- [12] H. Chen, B. Perozzi, Y. Hu, and S. Skiena, *HARP: Hierarchical representation learning for networks*, in *Proc. AAAI Conf.*, 2018.
- [13] T.A. Davis, W.W. Hager, S.P. Kolodziej, and S.N. Yeralan, *Algorithm 1003: Mongoose, a graph coarsening and partitioning library*, *ACM Trans. Math. Softw.*, 46 (2020).
- [14] T.A. Davis and Y. Hu, *The University of Florida sparse matrix collection*, *ACM Trans. on Mathematical Software*, 38 (2011).
- [15] I.S. Dhillon, Y. Guan, and B. Kulis, *Weighted graph cuts without eigenvectors a multilevel approach*, *IEEE Transactions on Pattern Analysis and Machine Intelligence*, 29 (2007), pp. 1944–1957.
- [16] H.C. Edwards, C.R. Trott, and D. Sunderland, *Kokkos: Enabling manycore performance portability through polymorphic memory access patterns*, *Journal of Parallel and Distributed Computing*, 74 (2014), pp. 3202–16.
- [17] B. Fagginger Auer, *GPU Acceleration of Graph Matching, Clustering, and Partitioning*, PhD thesis, Utrecht University, 2013.
- [18] B. Fagginger Auer and R.H. Bisseling, *Graph coarsening and clustering on the GPU*, *Graph Part. and Graph Clustering*, 588 (2012), p. 223.
- [19] M.S. Gilbert, S. Acer, E.G. Boman, K. Madduri, and S. Rajamanickam, *Performance-portable graph coarsening for efficient multilevel graph analysis*, in *Proc. IEEE Int’l. Parallel and Distributed Processing Symp. (IPDPS)*, 2021.
- [20] Y. Goldschmidt, M. Galun, E. Sharon, R. Basri, and A. Brandt, *Fast multilevel clustering*, tech. report, Weizmann Institute of Science, 2005.
- [21] B. Goodarzi, F. Khorasani, V. Sarkar, and D. Goswami, *High performance multilevel graph partitioning on gpu*, in *2019 International Conference on High Performance Computing & Simulation (HPCS)*, 2019, pp. 769–778, <https://doi.org/10.1109/HPCS48598.2019.9188120>.
- [22] L. Gottesbüren, T. Heuer, and P. Sanders, *Parallel Flow-Based Hypergraph Partitioning*, in *20th Int’l. Symp. on Experimental Algorithms (SEA)*, C. Schulz and B. Uçar, eds., vol. 233 of *Leibniz International Proceedings in Informatics (LIPIcs)*, Dagstuhl, Germany, 2022, Schloss Dagstuhl – Leibniz-Zentrum für Informatik, pp. 5:1–5:21, <https://doi.org/10.4230/LIPIcs.SEA.2022.5>.
- [23] L. Gottesbüren, T. Heuer, P. Sanders, C. Schulz, and D. Seemaier, *Deep multilevel graph partitioning*, in *29th Annual European Symposium on Algorithms, ESA 2021, September 6–8, 2021, Lisbon, Portugal (Virtual Conference)*, vol. 204 of *LIPIcs*, Schloss Dagstuhl -

- Leibniz-Zentrum für Informatik, 2021, pp. 48:1–48:17, <https://doi.org/10.4230/LIPIcs.ESA.2021.48>.
- [24] A. Heinlein, A. Klawonn, S. Rajamanickam, and O. Rheinbach, *FROSch: A fast and robust overlapping Schwarz domain decomposition preconditioner based on Xpetra in Trilinos*, Tech. Report SAND2018-13025R, Sandia National Laboratories, 2018, <https://doi.org/10.2172/1482862>.
- [25] B. Hendrickson and R. Leland, *The Chaco users guide. version 1.0*, tech. report, Sandia National Laboratories Albuquerque, 1993.
- [26] W. Hu, M. Fey, M. Zitnik, Y. Dong, H. Ren, B. Liu, M. Catasta, and J. Leskovec, *Open Graph Benchmark: Datasets for machine learning on graphs*, in Proc. Annual Conf. on Neural Inf. Proc. Systems, 2020.
- [27] Y. Hu and L. Shi, *Visualizing large graphs*, WIREs Computational Statistics, 7 (2015), pp. 115–136.
- [28] G. Karypis and V. Kumar, *A fast and high quality multilevel scheme for partitioning irregular graphs*, SIAM Journal on Scientific Computing, 20 (1998).
- [29] Y. Koren, L. Carmel, and D. Harel, *Drawing huge graphs by algebraic multigrid optimization*, Multiscale Modeling & Simulation, 1 (2003), pp. 645–673.
- [30] D. LaSalle and G. Karypis, *Multi-threaded graph partitioning*, in Proc. IEEE Int'l. Parallel and Distributed Processing Symp. (IPDPS), 2013.
- [31] D. LaSalle and G. Karypis, *A parallel hill-climbing algorithm for graph partitioning*, in Proc. Int'l. Conf. on Parallel Processing (ICPP), 2016.
- [32] D. LaSalle, M.M.A. Patwary, N. Satish, N. Sundaram, P. Dubey, and G. Karypis, *Improving graph partitioning for modern graphs and architectures*, in Proc. Workshop on Irregular Applications: Architectures and Algorithms (IA3), 2015.
- [33] A. Lenharth, D. Nguyen, and K. Pingali, *Parallel graph analytics*, Commun. ACM, 59 (2016), p. 78–87.
- [34] A. Pothen, *Graph partitioning algorithms with applications to scientific computing*, in Parallel Numerical Algorithms, Springer, 1997, pp. 323–368.
- [35] U.N. Raghavan, R. Albert, and S. Kumara, *Near linear time algorithm to detect community structures in large-scale networks*, Physical Review E, 76 (2007), p. 036106.
- [36] I. Safro, P. Sanders, and C. Schulz, *Advanced coarsening schemes for graph partitioning*, J. Exp. Algorithms, 19 (2015).
- [37] S. Sakr, A. Bonifati, H. Voigt, A. Iosup, K. Ammar, R. Angles, W. Aref, M. Arenas, M. Besta, P.A. Boncz, K. Daudjee, E.D. Valle, S. Dumbrava, O. Hartig, B. Haslhofer, T. Hegeman, J. Hidders, K. Hose, A. Iamnitchi, V. Kalavri, H. Kapp, W. Martens, M.T. Özsu, E. Peukert, S. Plantikow, M. Ragab, M.R. Ripeanu, S. Salihoglu, C. Schulz, P. Selmer, J.F. Sequeda, J. Shinavier, G. Szárnyas, R. Tommasini, A. Tumeo, A. Uta, A.L. Varbanescu, H.Y. Wu, N. Yakovets, D. Yan, and E. Yoneki, *The future is Big Graphs: A community view on graph processing systems*, Commun. ACM, 64 (2021), p. 62–71.
- [38] P. Sanders and C. Schulz, *Engineering Multilevel Graph Partitioning Algorithms*, vol. 6942 of Lecture Notes in Computer Science, Springer Verlag, 2011, p. 469–480, [https://doi.org/10.1007/978-3-642-23719-5\\_40](https://doi.org/10.1007/978-3-642-23719-5_40).
- [39] G.M. Slota, K. Madduri, and S. Rajamanickam, *PuLP: Scalable multi-objective multi-constraint partitioning for small-world networks*, in Proc. IEEE Int'l. Conf. on Big Data (Big Data), 2014.
- [40] B. Smith, P. Bjorstad, and W. Gropp, *Domain decomposition: parallel multilevel methods for elliptic partial differential equations*, Cambridge university press, 2004.
- [41] S.H. Teng, *Coarsening, sampling, and smoothing: Elements of the multilevel method*, in Algorithms for Parallel Processing, M.T. Heath, A. Ranade, and R.S. Schreiber, eds., Springer, 1999, pp. 247–276.
- [42] J. Xu and L. Zikatanov, *Algebraic multigrid methods*, Acta Numerica, 26 (2017), p. 591–721, <https://doi.org/10.1017/S0962492917000083>.